Proceedings of the ASME 2011 Pressure Vessels & Piping Division Conference
PVP2011
July 17-21, 2011, Baltimore, Maryland, USA

PVP2011-57955

MITIGATION OF DISTORTION IN AN EDGE-WELDED BAR BY CLAMPING PARAMETERS

Mahyar Asadi *

Mechanical and Aerospace Engineering
Carleton University
Ottawa, Ontario, K1S 5B6
Canada
masadi@connect.carleton.ca

John A. Goldak

Mechanical and Aerospace Engineering
Carleton University
Ottawa, Ontario, K1S 5B6
Canada
jgoldak@mrco2.carleton.ca

ABSTRACT

The objective is to demonstrate a capability developed to explore a design space to minimize distortion and evaluate the sensitivity of the distortion of an edge weld on a 152 x 1220 x 12.5 mm bar of Aluminum 5052-H32 wrt clamping. For each point in the design space, a full computational model that includes transient 3D thermal and stress analysis is solved using VrWeld software [1]. The bar has no displacement constraints other than rigid body constraints and the resulting camber from welding bends the bar. The minimum distortion in this discrete design space is assumed to be the optimal design to minimize the final distortion, i.e., objective function. The design space parameters chosen are clamping parameters, i.e., prescribed displacements, and the release time value in the design space. The bar is fixed at both ends and subjected to a range of prescribed displacements opposite to the direction of the camber. In the first set of tests the prescribed displacement is applied directly in the middle of the bar and in the second set of tests the displacement field is prescribed as a parabolic displacement along the full length of the bottom of the bar. In addition to the effect of the prescribed displacement on final distortion is shown to be highly correlated with the delay time at which the prescribed displacement is released after the weld is finished. The best pair of the prescribed value and the release time value in the design space. The distortion and residual stress fields in the mitigated bar with a nodal prescribed displacement in the middle of the bar and the mitigated bar with a parabolic prescribed displacement along the bottom surface of the bar are compared.

INTRODUCTION

Distortion in a weld results from inhomogeneous expansion and contraction of the weld metal and adjacent base metal during the heating and cooling cycle of the welding process. Heating and cooling involves significant local volumetric thermal strains that generate permanent plastic deformation. The cause of welding residual stress/distortion is the nonlinear behavior due to this plastic deformation [2] and [3].

Because distortion due to welding can increase fabrication costs and residual stress can reduce the in-service life due to fatigue or corrosion failures, designers would like to minimize their harmful effects. The usual classical approach would be to design a Design-Of-Experiment (DOE) test matrix and perform the physical experiments defined by the test matrix. This is expensive in time and money. Because the DOE test matrix is designed with limited information, understanding or insight of the design space, it may not be the optimal DOE matrix. This paper argues that given such a proposed DOE test matrix, there can be significant benefits from running a multiple computer simulation to evaluate all of the points in the design space that are defined by the DOE test matrix. This capability supports designers to construct and use more efficient DOEs.

In the authors' experience the cost of the computer simula-

*Address all correspondence to this author.

tion for CWM of industrial welding problems is less than 1% of the cost of the physical experiments and take less than one week which is much less than the time to perform the physical experiment. An automated machinery for multiple setups and analyses that saves user's time significantly in computer simulation for CWM of industrial welding problems, can implement larger and advanced DOEs in feasible time to support designer-driven optimization and control application of CWM.

In this paper the design space is chosen to demonstrate the this capability. The design parametres are prebending value and the delay time at which clamps or fixtures are released. Okerblom [4], Vinokurov [5], and Brust [6] discussed different techniques for mitigation of distortion from welding. One of the techniques is to use clamping or prebending. Very good simulation codes are now available to predict the behavior of a welded structure under clamping BCs based on welding heat distribution and stress-strain analysis for every node in domain. However these computer models have largely been limited to models that analyze a single instance of a weld or welded structure. This paper uses the parametric-design DOE for welds and welded structures that creates a single computer project to solve tens of computer models to explore or map the associated design space specified by a Design of Experiments (DOE) in order to find a minimum distortion in an edge-welded bar constrained by clamping functions. The authors' emphasize that the user clicks one 'run' button once to run all of the projects defined by the DOE matrix.

CWM AS A CONTROL PROBLEM

From a control point of view, we have a control problem with a large time-dependent vector Q that describes the state space of CWM at the time t. The state space is governed by CWM analysis written as a form in Eq. 1 where u is a control vector and F is a mapping from $R^m \rightarrow R^n$. R^m forms the control space and R^n is the state space.

$$Q_t = F\left(Q_{t-1}, u_t\right) \tag{1}$$

We also define a scalar-valued function ϕ called an objective function that is to be minimized/maximized. ϕ is a function of on the state space, Q, and control vector u. The state space, Q, is a function of the control vector u and therefore the function ϕ really depends only on u (See Eq. 2).

$$\phi\left(Q,u\right) = \phi\left(Q\left(u\right),u\right) = \phi\left(u\right) \tag{2}$$

The question that all optimization methods try to answer is how the objective function, ϕ, changes wrt changes in the control vector u. Optimization algorithms are usually described independent of the algorithm and machinery needed to evaluate the objective function. This paper focusses on the software machinery to evaluate the objective function which requires the associated state space to be evaluated. Therefore the choice of optimization algorithm is not the main focus of this paper.

Mapping from control space to the state space, i.e., CWM analysis, plays a critical role in the industrial applications of weld optimization problems. If the capability of such analysis exists to solve problems in a feasible time and cost, then the optimization is straight forward. A set of points in the control space can be defined in the form of a matrix in which each row defines one point in the design space and each column defines one coordinate or variable in the design space. This matrix is formally similar to a design of experiment (DOE) matrix. DOE is the terminology used in this paper to define the set of points in the design space that are to be evaluated. However in this paper, the analysis uses a deterministic model and there is no uncertainty in the solution other than truncation error and precision. Furthermore, the paper is not primarily concerned with how to chose the optimal DOE matrix. The focus of the paper is to demonstrate solving a given DOE matrix of CWM quickly at low cost with one 'click of the run' button.

COMPUTATIONAL MODEL

The full computational model that includes thermal and stress analysis are analyzed by VrWeld software [1]. The details of the model for transient thermal and stress analysis are described below. The Computational Weld Mechanics (CWM) model in VrWeld is validated in [7] by comparing the transient temperature, strain and deflection on this bar with the experimental data from [8].

An edge weld on a 152 x 1220 x 12.5 mm bar of Aluminium 5052-H32 shown in Fig. 1, was employed for validation in [7]. This edge-welded-bar test is used in this paper for exploring the clamping design space to mitigate the distortion on the bar. The mesh employed is shown in Fig. 2 has 6600 8-node brick elements and 9680 nodes.

The material was aluminum 5052-H32 alloy with chemical composition Al 96.7, Mg 2.5, Cr 0.25, Cu max 0.1, Fe max 0.4, Mn max 0.1, Si max 0.25, Zn max 0.1 Wt %. The temperature dependent material properties of Al 5052-H32 were given in [8] and this data was employed in the analysis of this test. The gas metal-arc-welding process was employed to weld the specimen and the welding parameters were current 260 amperes, voltage 23 volts, travel speed 7.34 mm/s, filler metal Al-4043 with 1.6 mm wire diameter, wire feed speed 170 mm/s and the shielding gas was Argon. The specimen was allowed to cool to ambient temperature after welding was completed.

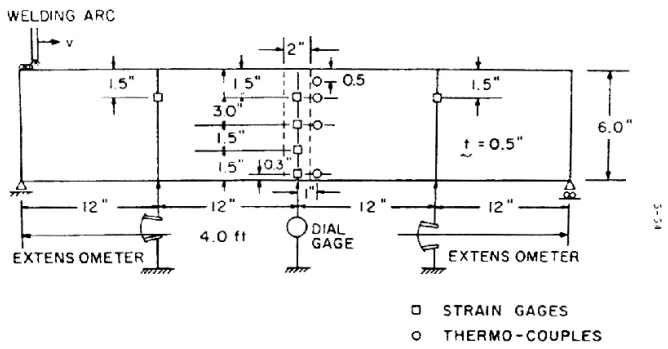

FIGURE 1. SPECIMEN VALIDATED AND USED IN THIS ANALYSIS.

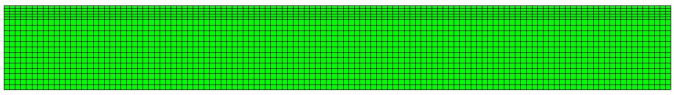

FIGURE 2. A 2D VIEW OF 3D MESH USED IN THIS ANALYSIS.

Thermal Analysis

The 3D transient temperature is computed by solving the transient heat equation.

$$\dot{h} + \nabla \cdot (-\kappa \nabla T) = Q \tag{3}$$

where h is the specific enthalpy, the super imposed dot denotes the derivative wrt to time, κ is the thermal conductivity, T is the temperature, and Q is the power per unit volume or the power density distribution.

The transient heat equation was solved with a Lagrangian finite element method [9]. The initial temperature was 300 $^{\circ}K$. The power density distribution function Q $[w/m^3]$, the 'Double Ellipsoid' heat source model [10], was used with the heat source sizes; front, rear, width and depth set to 8, 16, 10 and 8 mm (see Fig 3).

A convection boundary condition generated a boundary flux q $[w/m^2]$ on all external surfaces. This flux is computed from Eq. 4 with ambient temperature of T_{ambient} = 300 $^{\circ}K$ and convection coefficient as a function of temperature given in Eq. 5 extracted from [11] by interpolation of experimental data.

$$q = h_c(T - T_{\text{ambient}}) \tag{4}$$

$$h_c = 7.2 - \left(\frac{355000}{T^2}\right) + (0.001 \times T)\ [w/m^2K] \tag{5}$$

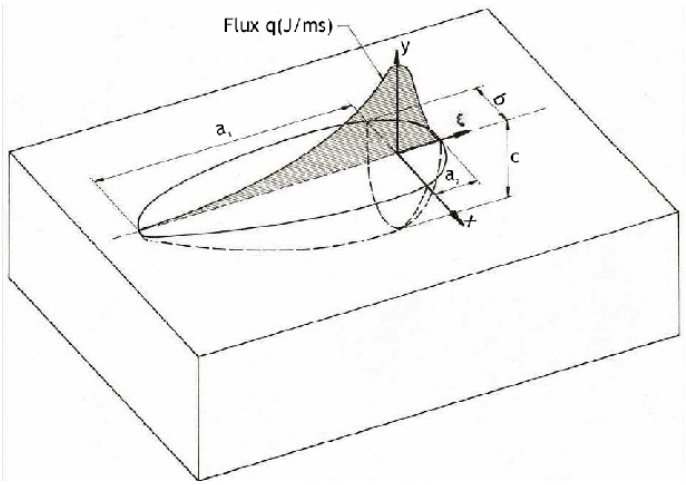

FIGURE 3. DOUBLE ELLIPSOID PARAMETERS; FRONT a_2, REAR a_1, WIDTH b, AND DEPTH c.

The time step length while welding was chosen so that in one time step the heat source was required to travel one element along the weld path. Filler metal was added as the welding arc moved along the weld path, i.e., the FEM domain changed in each time step during welding. After each weld pass was completed, the time step length was increased exponentially by a factor of 1.2 per time step until the the analysis was halted. The cool down time and the maximum temperature was 3600 seconds and 334 $^{\circ}K$ respectively when the analysis halted.

Stress Analysis

Given the density ρ, the elasticity tensor as a 6×6 matrix, the body force b and the Green-Lagrange strain ε, VrWeld solves the conservation of momentum equation that can be written in the form of Eq. 7 in which inertial forces, $\rho\ddot{x}$, are ignored.

$$\begin{aligned} \nabla \cdot \sigma + b &= 0 \\ \sigma &= D\varepsilon \\ \varepsilon &= (\nabla u + (\nabla u)^T + (\nabla u)^T \nabla u)/2 \end{aligned} \tag{6}$$

VrWeld solves this partial differential equation for a visco-thermo-elasto-plastic stress-strain relationship using theory and algorithms developed by J. C. Simo and his colleagues [12]. The initial state is assumed to be stress free. However, if the initial stress state was known, it could be initialized in VrWeld. The displacement boundary conditions for the test removed the rigid body modes by constraining the bottom left edge to zero displacement and to constrain the bottom right edge to zero transverse motion and zero vertical motion but allow horizontal translation.

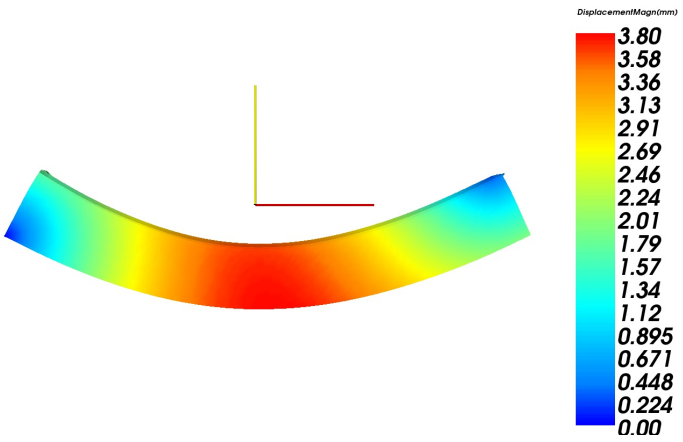

FIGURE 4. FINAL MAGNITUDE OF DISTORTION (50X). RED AND YELLOW AXIS SHOW POSITIVE X AND Y DIRECTION.

The system is solved using a time marching scheme with time step lengths of approximately 3 seconds during welding and usually an exponentially increasing time step length when welding stops.

OPTIMIZATION PROBLEM

When the part is free to deform but rigid body modes are constrained to zero, the final distortion forms a camber in the bar so that the maximum occurs in the middle of the bar as shown in Fig. 4. The maximum magnitude of Y displacement is 3.6 mm.

Prescribing a bending displacement equal and opposite to the camber in the unconstrained bar reduces the final distortion but does not eliminate it entirely. The amount of opposite prescribed camber that minimizes the final camber is one of the design parameters. Not only the magnitude of the prescribed displacement but also the way it is prescribed needs to be decided. One strategy is to apply the prescribed displacement in the middle of the bar to a series of nodes along the thickness. Another strategy choosen is to prescribe a parabolic shape of the bar in the direction to the camber to all nodes on the bottom surface of the bar. The effect of prescribed displacement on final distortion is highly correlated with the delay time when the prescribed displacement release after the weld is finished and it introduces another design parameter for clamping technique. Therefore each strategy is solved as an optimization problem and the design parameters are the magnitude of the prescribed displacement and the delay time of the prescribed displacement release after the weld is finished. The objective function is the L_∞ norm for the nodal displacements in the bottom line of the bar, i.e., the maximum distortion at the bottom of the bar

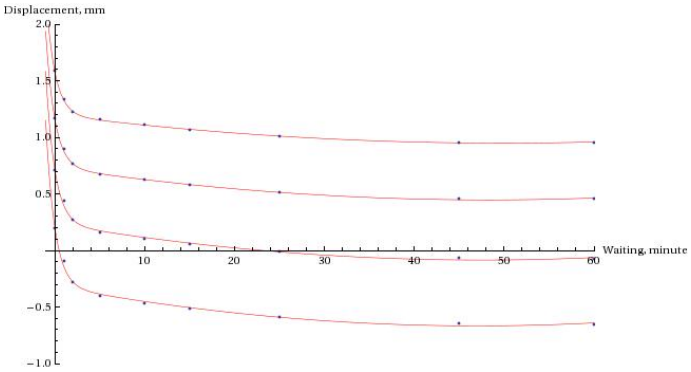

FIGURE 5. OBJECTIVE FUNCTION, I.E., MAXIMUM FINAL Y-DISPLACEMENT AT THE END OF THE PROCESS. EACH CURVE IS FITTED TO THE SET OF POINTS FOR ONE PRESCRIBED DISPLACEMENT.

Prescribed Displacement in the Middle

In this strategy, a prescribed displacement applied to a row of nodes in the bottom middle of the bar. Besides rigid body motion fixity, both bottom ends of the bar were fixed with zero Y displacement. Different values of prescribed displacement were applied to the row of nodes picked at the mid-point of the bar. These prescribed values were held during the welding plus a set of different delay time during the cool down to the ambient temperature. When the prescribed displacement was released, at least one time step computed the equilibrium stress state after releasing the fixities except for rigid body constraints. The design parameters; values of nodal prescribed displacement and delay time, have a quite large range of possible variation and therefore the design space is discretized by picking 5 values of nodal prescribed displacement and 9 delay times resulting in 45 nodes in the discrete design space. A full factorial DOE including the 45 nodes, was used to give a fully-covered map of the design parameters. Table 1 shows the DOE employed and the evaluated objective function for each point of design space tested. This is shown in form of plot in Fig. 5 where each curve illustrates a fitted curve for one prescribed displacement for the whole range of delay time from zero to one hour, i.e, total process time. The fitted curve equations are given in Eq. 7, 8, 9 and 10. Total analysis for each design point takes 48 minutes and using 4 cores, the DOE finished in 9.6 hours and the minimum displacement of about zero was computed with no need to refine the discretization of the design space.

$$Y = 0.0001t^2 - 0.01t + 0.39e^{-t} + 1.2 \tag{7}$$

$$Y = 0.0001t^2 - 0.01t + 0.44e^{-t} + 0.7 \tag{8}$$

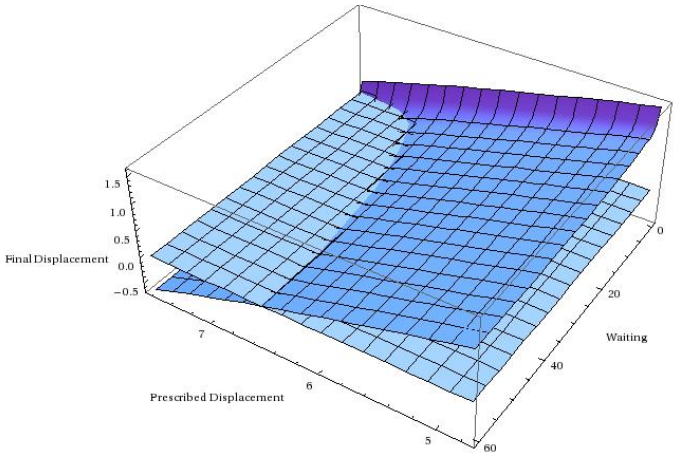

FIGURE 6. FINAL Y-DISPLACEMENT TATE SPACE VS. THE PRESCRIBED DISPLACEMENT AND THE DELAY TIME ACHIEVED FOR THE NODAL PRESCRIBED DISPLACEMENT AT THE END OF PROCESS AND ZERO FINAL DISPLACEMENT SURFACE INTERSECT IT.

$$Y = 0.0001t^2 - 0.01t + 0.49e^{-t} + 0.2 \tag{9}$$

$$Y = 0.0001t^2 - 0.01t + 0.53e^{-t} - 0.3 \tag{10}$$

Y : Objective function in mm.
t : Delay time in minute.

The curves in Fig. 5 were plotted in 3D form and intersected with a flat plane of zero displacement as illustrated in Fig. 6. The intersection of the two smooth surfaces is a curve shown in Fig. 7 and the fitted equation to the node picked on the intersection curve, is given in Eq. 11. This curve or equation shows all points in the state surface with zero final zero displacement.

$$d = 0.0002t^2 - 0.02t + 1.36e^{-t} + 6.98 \tag{11}$$

d : Prescribed nodal displacement required to achieve zero final displacement in mm.
t : Delay time required to achieve zero final displacement in minute.

Parabolic Displacement at the bottom

In this strategy, a parabolic Y-displacement similar but opposite of the Y-displacement in the unconstrained bar is applied to all nodes at the bottom of the bar. The parabolic function given in Eq. 12 is zero at both ends and equals h at the middle of the

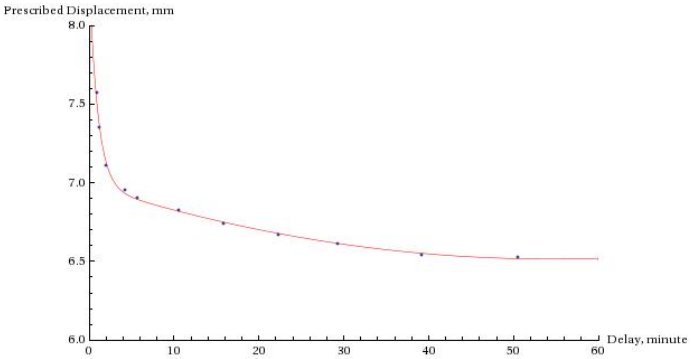

FIGURE 7. THE CURVE SHOWS THE PRESCRIBED DISPLACEMENT MAGNITUDE AND DELAY TIME REQUIRED TO ACHIEVE ZERO FINAL DISPLACEMENT.

bar. Different values of h were applied and held during the welding plus a set of different delay times during the cool down to the ambient temperature. When the prescribed displacement was released, at least one time step computed the equilibrium stress state after releasing the fixities except for rigid body constraints.

$$Displ. = h\left(1 + \frac{X}{L}\right)\left(1 - \frac{X}{L}\right) \tag{12}$$

Displ. : Prescribed displacement function.
h : Maximum displacement in the middle of the bar.
X : Position in the bar varing from -L to L.
L : Bar's haf-length.

The DOE is similar to the nodal prescribed displacement test using a meshed space of design parameters with 5 parabolic h values and 9 delay times. The upper and lower bounds are different for the parabolic prescribed displacement test. Employing 4 cores and having a DOE with the 44 nodes (divisible by 4) saves CPU time. Therefore from the behavior observed in the nodal prescribed displacement test, one node with a low probability of minimum is deleted and a DOE matrix of size 44 is used. This DOE given in Table 2, finished in 8.8 hours and the zero minimum was found accurately with no need to refine the mesh of the design parameter space.

Fig. 8 illustrates fitted curves for each h value for the whole range of delay times. The fitted curve equations are given in Eq., 14, 15 and 16.

$$Y = 0.0001t^2 - 0.01t + 0.37e^{-t} + 1.06 \tag{13}$$

$$Y = 0.0001t^2 - 0.01t + 0.40e^{-t} + 0.41 \tag{14}$$

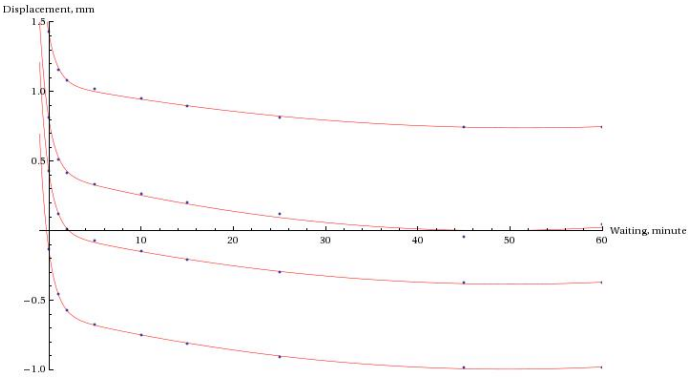

FIGURE 8. OBJECTIVE FUNCTION, I.E., MAXIMUM FINAL Y-DISPLACEMENT AT THE END OF THE PROCESS. EACH CURVE IS FITTED TO THE SET OF POINTS FOR ONE h VALUE.

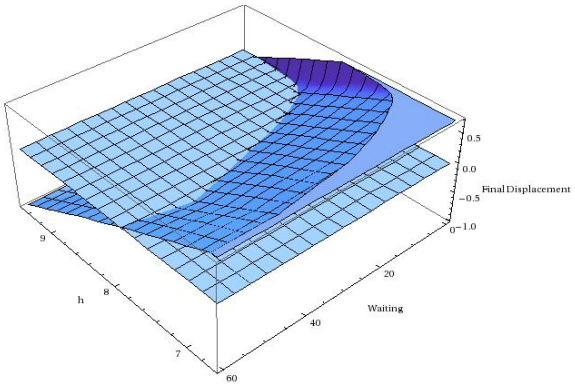

FIGURE 9. FINAL Y-DISPLACEMENT TATE SPACE VS. h VALUE AND THE DELAY TIME ACHIEVED FOR THE NODAL PRESCRIBED DISPLACEMENT AT THE END OF PROCESS AND ZERO FINAL DISPLACEMENT SURFACE INTERSECT IT.

$$Y = 0.0001t^2 - 0.01t + 0.45e^{-t} - 0.02 \qquad (15)$$

$$Y = 0.0001t^2 - 0.01t + 0.47e^{-t} - 0.61 \qquad (16)$$

Y : Maximum final displacement achieved at the end of process in mm.
t : Delay time in minute.

The curves in Fig. 8 were plotted in 3D form and intersected with a flat surface of zero displacement as illustrated in Fig. 9. The intersection of the two smooth surfaces is the curve shown in Fig. 10 and the fitted equation to the node picked on the intersection line, is given in Eq. 17. This curve or equation shows h as a function of the the delay time required to achieve zero final displacement on the bar.

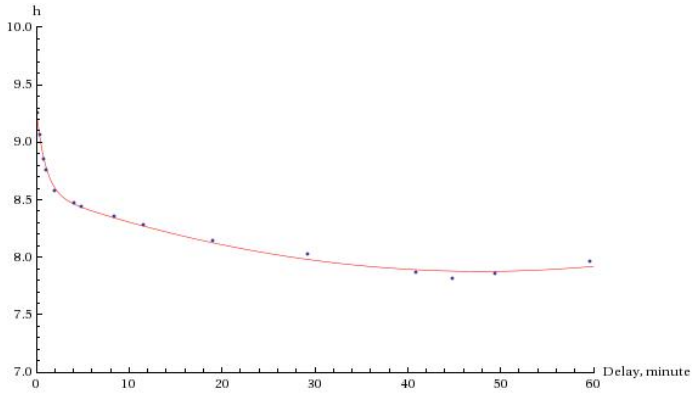

FIGURE 10. THE CURVE SHOWS h VALUE AND DELAY TIME REQUIRED TO ACHIEVE ZERO FINAL DISPLACEMENT.

$$h = 0.0003t^2 - 0.03t + 0.73e^{-t} - 8.56 \qquad (17)$$

h : Prescribed h required to achieve zero final displacement in mm.
t : Delay time required to achieve zero final displacement in minute.

CWM RESULTS

The deflection and residual stress are interesting for designer of welded structures. Fig. 11 compares the final deflection for the two mitigation strategies discussed. Distance is from the left bottom corner to the right bottom corner of the bar and units are meter. For prebending with prescribed deflections applied at the mid-point of the lower edge, the reaction forces or Lagrange multipliers are concentrated loads that generate local plastic deformation.

Fig. 12 compares the longitudinal residual stress in the bar for the two mitigation strategies after welding is complete. Residual stress is plotted for a line normal to the weld from the top edge to the bottom edge of the bar at the mid-length of the bar. Units are Pa and m for stress and distance respectively. For prebending with prescribed deflections applied at the mid-point of the lower edge, the reaction forces or Lagrange multipliers generate plastic strain and a very high residual stress at the bottom edge of the bar. For this case, the longitudinal residual stress in the weld has the highest compressive stress of the mitigation methods.

It would be a simple matter to solve a DOE to minimize longitudinal residual stress after welding was complete and the bar cooled to room temperature if one chooses an objective function. The question is what objective function to choose? Two possible choices are the maximum tensile residual stress or the

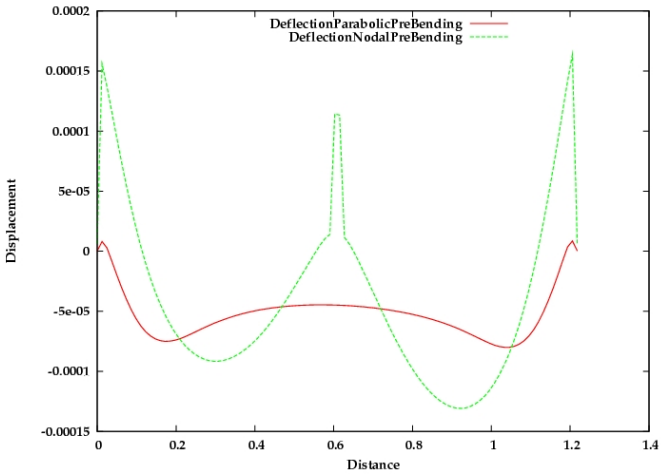

FIGURE 11. FINAL DEFLECTION FROM THE TWO MITIGATION STRATEGIES EMPLOYED. DISTANCEIS FROM THE LEFT BOTTOM CORNER TO THE RIGHT BOTTOM CORNER OF THE BAR. UNITS ARE m.

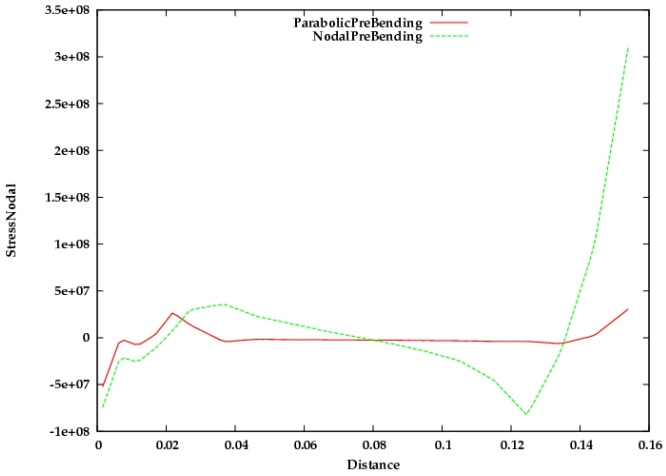

FIGURE 12. LONGITUDINAL RESIDUAL STRESS FROM THE TWO MITIGATION STRATEGIES EMPLOYED. THIS IS PLOTTED FOR A LINE NORMAL TO THE WELD FROM THE TOP EDGE TO THE BOTTOM EDGE OF THE BAR IN THE MID-LENGTH. UNITS ARE Pa AND m.

integral of the square of the longitudinal stress over the cross-section $\int_0^W \sigma_{xx}^2 dW$ where W is the width of the bar. There are many other possible objective functions. Which metric is preferred would depend on the requirements the designer is trying to satisfy. It is also possible to have multiple objective functions and compute the Pareto optimal solutions.

CONCLUSION

A Design of Experiments (DOE) matrix is used to define a set of points in the design space to be evaluated in order to find a minimum distortion in the bar for various clamping parameters. The set of points in the design space defined by the DOE matrix are evaluated by the software as a single problem with the DOE matrix as an input file to the software. This is quite different from the user using the DOE matrix to separately create and separately solve one project for each row of the DOE matrix.

In this paper, the user sets up only one reference or base project and one DOE matrix with 45 design points. This ran as a single project that analyzed all 45 design points in 9.6 CPU hours on a single core of a 3.3 GHZ Intel quad-core processor. With the same base project, a second DOE matrix was created with 44 design points. This analysis required 8.8 CPU hours. The user spends no time to set up the analysis for any design point other than the design point for the base or reference project. In addition, the results and post-processing are all structured for each DOE matrix. In the authors' experience, it would takes weeks of an expert user's time to set up the 89 projects for these two DOEs. Furthermore, managing post-processing would be difficult, time consuming and prone to error.

For each point in the design space, the transient thermal and displacement fields are computed. To demonstrate the capability of a single run of a complete DOE matrix, this paper uses a parametric-design DOE matrix of the welds and welded structures to explore or map the associated design space in order to find a minimum distortion by clamping parameters. This methodology could be applied to any welded structure to explore any set of points in a design space specified by a DOE matrix as a single project in which the variables are parameters of the computational model.

ACKNOWLEDGMENT

The authors would like to thank Daniel Downey, Stanislav Tchernov and Jianguo Zhou for their support and contribution to this study. The authors are grateful to referees for their comments that led to improvements in this paper. The financial support of the National Science and Engineering Research Council (NSERC) is gratefully acknowledged.

TABLE 1. DOE EMPLOYED FOR PRESCRIBED DISPLACEMENT IN THE MIDDLE OF THE BAR. PLOTS IN FIG. 5.

Test No.	Nodal P. Displ. (mm)	Delay Time (min)	Obj. Func. (mm)
1	3.80	0	2.04
2	3.80	1	1.80
3	3.80	2	1.71
4	3.80	5	1.65
5	3.80	10	1.60
6	3.80	15	1.57
7	3.80	25	1.51
8	3.80	45	1.46
9	3.80	60	1.46
10	4.75	0	1.59
11	4.75	1	1.33
12	4.75	2	1.22
13	4.75	5	1.16
14	4.75	10	1.11
15	4.75	15	1.07
16	4.75	25	1.01
17	4.75	45	0.96
18	4.75	60	0.96
19	5.70	0	1.16
20	5.70	1	1.00
21	5.70	2	0.77
22	5.70	5	0.68
23	5.70	10	0.62
24	5.70	15	0.58
25	5.70	25	0.51
26	5.70	45	0.46
27	5.70	60	0.46
28	6.67	0	0.71
29	6.67	1	0.44
30	6.67	2	0.27
31	6.67	5	0.16
32	6.67	10	0.10
33	6.67	15	0.06
34	6.67	25	-0.01
35	6.67	45	-0.01
36	6.67	60	-0.01
37	7.60	0	0.20
38	7.60	1	-0.0
39	7.60	2	-0.02
40	7.60	5	-0.04
41	7.60	10	-0.04
42	7.60	15	-0.05
43	7.60	25	-0.05
44	7.60	45	-0.06
45	7.60	60	-0.06

TABLE 2. DOE EMPLOYED FOR PARABOLIC PRESCRIBED DISPLACEMENT. PLOTS IN FIG. 8.

Test No.	Parab. P. Displ. (mm)	Delay Time (min)	Obj. Func. (mm)
Del.	5.70	0	-
1	5.70	1	1.69
2	5.70	2	1.67
3	5.70	5	1.59
4	5.70	10	1.53
5	5.70	15	1.45
6	5.70	25	1.33
7	5.70	45	1.26
8	5.70	60	1.27
9	6.67	0	1.43
10	6.67	1	1.15
11	6.67	2	1.08
12	6.67	5	1.02
13	6.67	10	0.95
14	6.67	15	0.90
15	6.67	25	0.81
16	6.67	45	0.75
17	6.67	60	0.75
18	7.86	0	0.82
19	7.86	1	0.51
20	7.86	2	0.41
21	7.86	5	0.34
22	7.86	10	0.26
23	7.86	15	0.20
24	7.86	25	0.12
25	7.86	45	-0.01
26	7.86	60	0.01
27	8.55	0	0.43
28	8.55	1	0.12
29	8.55	2	0.01
30	8.55	5	-0.01
31	8.55	10	-0.14
32	8.55	15	-0.21
33	8.55	25	-0.30
34	8.55	45	-0.37
35	8.55	60	-0.37
36	9.50	0	-0.13
37	9.50	1	-0.46
38	9.50	2	-0.57
39	9.50	5	-0.67
40	9.50	10	-0.75
41	9.50	15	-0.81
42	9.50	25	-0.90
43	9.50	45	-0.98
44	9.50	60	-0.98

REFERENCES

[1] Goldak Technology Inc., *http://www.goldaktec.com/vrweld.html*, Accessed March 2011.

[2] Lincoln Electric Co. *http://www.lincolnelectric.com/knowledge/articles/content/distortion.asp* Accessed April 2010.

[3] D. Radaj, Welding Residual Stresses and Distortion; Calculation and Measurement, Revised edition, DVS Verlag, ISBN 3-87155-791-9, 2002.

[4] N. O. Okerblom, The Calculations of Deformations of Welded Metal Structures, Department of Scientific and Industrial Research, London, Translation from Russian, 1958.

[5] V. A. Vinokurov, Welding Stresses and Distortion: Determination and Elimination, The British Library Board 1977, Translated by J. E. Baker from Russian, 1968.

[6] Y. P. Yang, F. W. Brust, Z. Cao, Y. Dong, A. Nanjundan, Welding-induced distortion control techniques in heavy industries, 6th International Conference: Trends in Welding Research; Pine Mountain, GA; USA; 15-19 Apr. 2002. pp. 844-849. 2003.

[7] M. Asadi, J. A. Goldak, Challenges in Verification of CWM Software to Compute Residual Stress and Distortion in Weld, Proceeding of the ASME 2010 Pressure Vessel and Piping Division Conference, Bellevue, Washington, PVP2010-25770, July 18-22, 2010.

[8] K. Masabuchi, Analysis of Welded Structures, Section Transient Thermal Stress, pp.172 - 187, 1983.

[9] O. Zienkiewicz, R. Taylor, The Finite Element Method, Fourth Edition, Volume 2, McGraw-Hill, 1989.

[10] J. A. Goldak, A. Chakravarti, M. J. Bibby, A New Finite Element Model for Welding Heat Sources, Trans. AIME.186 Vol. 15B, pp. 299-305, June 1984, .

[11] J. D. Francis, Welding Simulations of Aluminum Alloy Joints by Finite Element Analysis, M. Sc. thesis Virginia Polytechnic Institute and State University, April 2002.

[12] J. C. Simo, Numerical Analysis of Classical Plasticity, Handbook for Numerical Analysis, Volume VI, ed. by P.G. Ciarlet and J.J. Lions, Elsevier, Amsterdam, 1998.